CO$_2$ adsorption by activated templated carbons

Marta Sevilla and Antonio B. Fuertes[*]

Instituto Nacional del Carbón (CSIC), P.O. Box 73, 33080 Oviedo, Spain

Abstract

Highly porous carbons have been prepared by the chemical activation of two mesoporous carbons obtained by using hexagonal- (SBA-15) and cubic (KIT-6)-ordered mesostructured silica as hard templates. These materials were investigated as sorbents for CO$_2$ capture. The activation process was carried out with KOH at different temperatures in the 600-800ºC range. Textural characterization of these activated carbons shows that they have a dual porosity made up of mesopores derived from the templated carbons and micropores generated during the chemical activation step. The activation process gives rise to an increase of the surface area and pore volume from 1020 m$^2 \cdot$g^{-1} and 0.91 cm$^3 \cdot$g^{-1} for the CMK-8 carbon to a maximum of 2660 m$^2 \cdot$g^{-1} and 1.38 cm$^3 \cdot$g^{-1} for a sample activated at 800 ºC (KOH/CMK-8 mass ratio of 4). Irrespective of the type of templated carbon used as precursor or the operational conditions used for the synthesis, the activated samples exhibit similar CO$_2$ uptake capacities, of around 3.2 mmol CO$_2$ g^{-1} at 25 ºC. The CO$_2$ capture capacity seems to depend on the presence of narrow micropores (<1 nm) rather than on the surface area or pore volume of activated carbons. Furthermore, it was found that these porous carbons exhibit a high CO$_2$ adsorption rate, a good selectivity for CO$_2$–N$_2$ separation and they can be easily regenerated.

---

[*] Corresponding author. Tel: 34 985 119090. E-mail address: abefu@incar.csic.es (A. B. Fuertes)

1. Introduction

The mitigation of the anthropogenic CO_2 emissions generated by the combustion of fossil fuels is extremely important in view of the significant role that this gas plays in global climate change. For the reduction of carbon dioxide emissions from fixed-point sources, CO_2 capture and storage is the prevailing strategy [1]. In this respect, the absorption of this gas by means of alkanolamine solvents is a well-proved technology that can be used for large-scale separation of carbon dioxide [2]. However, this process suffers from several drawbacks (e. g. energy consumption, corrosion of the equipment, toxicity, etc) that hamper its implementation. It is therefore highly desirable to develop alternative capture methods. A promising option is the use of highly porous solids as sorbents for capturing CO_2 by means of pressure, temperature or vacuum swing adsorption systems [3-9]. In this respect, various porous adsorbents such as zeolites, metal-organic frameworks (MOFs), porous carbons or organic-inorganic hybrid sorbents have been considered as potential candidates for CO_2 capture [10-12].

Among the sorbents mentioned so far, activated carbons have revealed several advantages in terms of cost, availability, large surface area, an easy-to-design pore structure, hydrophobicity and low energy requirements for regeneration [7, 10, 11, 13-15]. However, most activated carbons exhibit low CO_2 uptakes, which limits their performance for this application. In order to improve the CO_2-adsorption capacity of activated carbons, two different strategies have been adopted. One simple approach consists in the incorporation of superficial basic sites that enhance the interaction of CO_2 (acidic gas) with the carbon surface. Currently, these basic sites consist in nitrogen functional groups incorporated through the reaction of porous carbon with different nitrogen-containing compounds (e. g. ammonia, amines, etc) [16, 17]. Recently, several authors have investigated a simpler route for the creation of basic centres which consists

in the use of nitrogen-rich compounds as precursors for the fabrication of N-doped carbons [18]. Another strategy that has been investigated to enhance the CO_2 capture capacity is the fabrication of porous carbons with a pore structure suitable for the CO_2 adsorption [19]. Recent research works have shown that activated carbons with a large population of pores of size 1–2 nm exhibit a better CO2 adsorption performance than those with narrower micropores or with a mesoporous pore network [19–21]. Porous carbons with these pore characteristics can be obtained via the chemical activation of different types of precursors with KOH. Recently, we reported the preparation of highly activated carbons with KOH using polypyrrole and hydrothermally carbonized biomass as precursors [20,21]. These activated carbons have a well-developed porosity with a large number of pores in the 1–2 nm range and they exhibit high CO_2 adsorption uptakes.

In the last decade, mesoporous templated carbons (MTCs) obtained by hard- or soft-templating routes have attracted widespread interest due to their unique pore characteristics, i.e., an ordered porosity primarily made up of uniform mesopores whose diameters can be tuned between 2 nm and 10 nm. In particular, these materials are useful as adsorbents of bulky molecules (i.e., dyes), as carriers for the immobilization of enzymes and other large biomolecules, as catalytic supports, in energy storage applications (i.e., supercapacitors) or as substrates for the insertion of inorganic substances with electrochemical properties (i.e., Li-ion batteries). However, in comparison with the activated carbons, MTCs contain a small number of micropores (<2 nm) that bars them from certain applications where the presence of this type of pores is essential (i.e., H_2 storage). To overcome this drawback, several authors have investigated the creation of micropores in MTC materials by means of a post-synthesis chemical activation treatment [22, 23]. The resulting activated templated carbons (ATC)

exhibit a dual porosity made up of mesopores and wall confined micropores of around 1–2 nm, which are generated during the chemical activation step. These activated carbons exhibit, in relation to MTC materials, more enhanced properties suitable for the applications such as H_2 storage or as supercapacitor electrodes [24,25]. Given the dual pore nature of ATC materials, they can be expected to make excellent sorbents for CO_2 capture. In the present work, we explore the CO_2 adsorption capacity of chemically activated templated carbons. We employed as precursors two templated carbons (i.e., CMK-3 and CMK-8) prepared by means of a hard-templating route by using two mesostructured silica materials as hard templates, i.e., SBA-15 and KIT-6, respectively. The chemical activation was performed with KOH. The CO_2 adsorption capacity was tested at different temperatures and at pressures in the 0–1 bar range. The rate of CO_2 adsorption, their selectivity toward CO_2–N_2, and the regenerability of ATC materials were also examined.

2. Experimental

2.1. Preparation of materials

2.1.1 Synthesis of templated carbons

CMK-3 and CMK-8 mesoporous carbons – inverse replicas of hexagonally and cubic-ordered mesoporous silica, SBA-15 and KIT-6, respectively – were prepared according to the procedure reported elsewhere [26]. The SBA-15 silica was synthesized according to the procedure reported by Zhao et al. [27], while the KIT-6 silica was prepared as described by Kleitz et al. [28]. The synthesis of the carbons was performed according to a procedure reported elsewhere [29]. Briefly, the mesostructured silica was impregnated with paratoluene sulfonic acid (>98%, Aldrich) (0.5 M in ethanol) for 1 h, filtered,

washed with a small volume of ethanol, and dried at 80 ºC. Afterward, furfuryl alcohol (>98%, Merck) was infiltrated into the porosity of the silica. The impregnated samples were cured in air for 8 h at 80 ºC in order to polymerize the furfuryl alcohol and to convert it into polyfurfuryl alcohol. It was then carbonized under nitrogen at 700 ºC (3 ºC min^{-1}). The sample was held for 1 h at this temperature. To obtain pure carbon samples, the resulting carbon–silica composite was immersed in 48% HF at room temperature for 15 h in order to remove the silica framework. The carbon samples obtained in the form of an insoluble fraction were washed with distilled water and then dried in air at 120 ºC.

2.1.2. Chemical activation of templated carbons

The templated carbons (CMK-3 and CMK-8) were chemically activated by heating a carbon-KOH mixture (KOH/carbon at a weight ratio of 2 or 4) under N_2 up to a temperature in the 600-800 ºC range (heating rate: 3 ºC/min, holding time: 1 h). The activated samples were then thoroughly washed several times with HCl (10 wt %) to remove any inorganic salts and then washed with distilled water until neutral pH. Finally, the activated carbon was dried in an oven at 120 ºC. The activated carbons thus synthesized were denoted as AT*X-y-z*, where *X* designates the type of templated carbon (*X=S* for CMK-3 and *X=K* for CMK-8), *y* the KOH/carbon weight ratio and *z* the activation temperature (in ºC).

2.2. Characterization of materials

Low-angle range X-ray diffraction (XRD) patterns were obtained on a Siemens D5000 instrument operating at 40 kV and 20 mA, using CuKα radiation. The morphology of the samples was examined by Scanning Electron Microscopy (SEM) using a Zeiss DSM 942 microscope. Transmission electron micrographs (TEM) were taken on a JEOL

(JEM-2000 FX) apparatus operating at 160 kV. The nitrogen sorption isotherms and textural properties of the carbons were determined at -196 ^{o}C using a conventional volumetric technique (Micromeritics ASAP 2020). The surface area was calculated by the BET method from the adsorption data obtained in the relative pressure (p/p$_{o}$) range of 0.04 to 0.2. The total pore volume was determined from the amount of nitrogen adsorbed at p/p$_{o}$=0.99. The pore size distribution (PSD) was calculated *via* a Non Local Density Functional Theory (NLDFT) method using nitrogen adsorption data and assuming a slit pore model. The micropore surface area and total micropore volume (pore size < 2 nm) were obtained *via* t-plot analysis. The volume of the narrow micropores (< 0.7 mm) was determined by applying the Dubinin-Radushkevitch (D-R) equation to the CO_2 adsorption data at 0 ^{o}C [29].

2.3. CO_2 adsorption measurements

CO_2 adsorption was measured using a Nova 4200e (Quantachrome) static volumetric analyzer. Prior to the adsorption analysis, the sample (around 50-100 mg) was degassed at 150 ^{o}C for several hours. The CO_2 adsorption experiments were performed at three temperatures: 0 ^{o}C, 25 ^{o}C and 50 ^{o}C.

The adsorption kinetics of CO_2 and N_2, and adsorption-desorption cycles were measured in a thermogravimetric analyser (C. I. Electronics). Both sets of experiments were performed at 25 ^{o}C and the temperature was controlled by means of a circulating bath (Haake K15). For the kinetic analysis, the sample (~ 10 mg) was degassed under a He stream at 200 ^{o}C for 1 hour. The gas was then switched from He to CO_2 or N_2 (100 mL·min^{-1}) and the weight variation with time was recorded. In the case of the adsorption-desorption cycles, the sample (~ 30 mg) was degassed under a stream of He at a temperature of 200 ^{o}C before the cyclic experiments. During the adsorption, the carbon sample was exposed to a stream of pure CO_2 (100 mL·min^{-1}). Once the sample

was saturated, the gas was switched from CO_2 to He (100 mL·min^{-1}) and the carbon dioxide was desorbed. This adsorption-desorption cycle was repeated several times.

3. Results and discussion

3.1. Structural characteristics of the chemically activated templated carbons

The structural properties of the templated and activated carbon materials were investigated by SEM, TEM, X-ray diffraction analysis and gas adsorption measurements. The SBA-15 silica is formed by rice-like particles (length $\sim$ 1 μm), whereas KIT-6 silica consists of large irregular particles of up to 50 μm. This morphology is preserved in the templated carbons as revealed by the insets in Figures 1a and 1b for the CMK-8 and CMK-3 samples respectively. Furthermore, these templated carbons exhibits the characteristic well-ordered mesoporous structure [31, 32], as can be inferred from the well-defined XRD patterns at the low angle range (see Fig. 2). This result is confirmed by the TEM images shown in Figures 1a and 1b, which correspond to the CMK-8 and CMK-3 samples, respectively.

Chemical activation of the templated carbons causes a change in their mesoporous structure. Indeed, the TEM images in Fig. 1 clearly show that the highly ordered mesoporous structure of the MTC samples gradually disappears with activation. This is confirmed by the XRD patterns, in which a gradual decrease in the intensity of the main XRD peak is observed as the activation proceeds (see Fig. 2). However, in spite of the loss of structural ordering caused by the chemical activation process, a certain order in the mesoporous structure of the activated carbons is still apparent.

The nitrogen sorption isotherms and corresponding pore size distributions (PSDs) for the activated carbons and templated carbons (i.e., CMK-3 and CMK-8) are

displayed in Fig. 3. The textural properties of these porous carbons are listed in Table 1. The sorption isotherms of the templated carbons exhibit a well-defined capillary condensation step that indicates that the porosity is mostly made up of uniform mesopores, as is confirmed by the pore size distributions (see Fig. 3b and d). Indeed, these samples exhibit narrow PSDs (~3.8 nm). By applying the D–R (Dubinin–Raduskevitch) method to the CO_2 adsorption data obtained at 0 ºC, we deduced that the CMK-3 sample has a micropore volume of 0.28 cm^3 g^{-1}. This can be ascribed to the intrinsic porosity of the carbonized polymer (i.e., polyfurfuryl alcohol), that is made up of very narrow micropores (<1 nm).

Whereas the MTC samples exhibit type IV sorption isotherms, the MTC-based activated carbons show a type I isotherm with a wide knee, which is characteristic of materials with a micro-mesoporous network (see Figures 3a and 3c). This change in the shape of the isotherms indicates changes in the porous structure, in particular the creation of a large number of micropores. Indeed, the PSDs shown in Figure 3b and 3d reveal that the porosity of the activated carbons is made up of two pore systems: i) one of them is formed by mesopores corresponding to those present in the templated carbons and ii) the second pore system consist of micropores (~ 1.2 nm) generated by KOH activation. As can be deduced from the data listed in Table 1, a remarkable increase of both the BET surface area and the pore volume takes place with the progress of activation (i. e. by increasing the reaction temperature or the KOH/MTC mass ratio). Most of the surface area and pore volume is associated to the micropores generated as consequence of KOH activation. As an example, for the AKT-4-800 sample around 80 % of the surface area (2660 $m^2 \cdot g^{-1}$) and pore volume (1.38 $cm^3 \cdot g^{-1}$) can be ascribed to the micropores.

The chemical activation process gives rise to the gasification of a certain amount of the carbon present in the MTC samples. Carbon loss increases with the reaction temperature or the amount of activating agent. In the samples prepared from CMK-3, the yield of activated carbon falls from 92 % (ATS-2-650) to 49 % (ATS-4-800) as indicated in Table 1.

3.2. CO_2 capture capacity

The CO_2 adsorption capacities of the porous carbons were investigated at three temperatures (0 ºC, 25 ºC and 50 ºC). A comparative analysis of the CO_2 adsorption isotherms (measured at 25 ºC) of two representative ATC samples (i. e. ATS-2-700 and ATK-2-700), a commercial activated carbon (M-30) and the CMK-3 templated carbon is presented in Figure 4. It can be seen that the CO_2 capture capacities of the ATCs are quite substantial and similar (~ 3.2 mmol $CO_2 \cdot g^{-1}$ at 25 ºC), and more important, they exhibit a superior CO_2 performance in relation to the other porous carbons. Moreover, this comparative analysis reveals that the activation process greatly enhances the CO_2 adsorption uptake of the ATC samples in relation to the pristine templated carbons. It should also be noted that, although the commercial activated carbon (M-30) displays a larger pore development than the ATC carbons (see Table 1), it exhibits a considerably lower adsorption capacity (2.2 mmol $CO_2 \cdot g^{-1}$). This result demonstrates that the capture capacity of the sorbents does not depend solely on textural properties such as the BET surface area or pore volume but also on the pore size distribution as we have already reported for other activated carbons [20, 21]. It is essential to bear this in mind when designing CO_2 carbon sorbents.

Table 2 summarizes the CO_2 capture capacities of the porous carbons. The activated templated carbons exhibit CO_2 uptakes which are comparable regardless of the activating conditions or on the type of pristine templated carbon. Indeed, most of the

capture capacities at adsorption temperatures of 0 ºC and 25 ºC are in the 4.9-5.8 mmol $CO_2 \cdot g^{-1}$ and 2.9-3.4 mmol $CO_2 \cdot g^{-1}$ ranges respectively. Interestingly, the CO_2 capture capacities are quite similar irrespective of the BET surface areas or pore volumes. As an example, the samples ATK-2-700 (S_{BET}=1450 $m^2 \cdot g^{-1}$, V_p=0.81 $cm^3 \cdot g^{-1}$) and ATK-4-800 (S_{BET}=2660 $m^2 \cdot g^{-1}$, V_p=1.38 $cm^3 \cdot g^{-1}$) exhibit similar CO_2 uptakes (~ 3.1 mmol $CO_2 \cdot g^{-1}$ at 25ºC) in spite of the large differences in the textural properties. These results indicate that the amount of CO_2 adsorbed bears no relation to the textural properties (i. e. BET surface area or pore volume). In earlier works, we demonstrated that the amount of CO_2 adsorbed mostly depends on the population of narrow micropores (< 1 nm), which make a considerable contribution to CO2 capture. This is due to the fact that micropores have a high adsorption potential that enhances the adsorption of CO_2 molecules. The CO_2 adsorption isotherms of the activated carbon samples prepared from CMK-3 are shown in Figure 5. It can be seen that the amount adsorbed decreases as the adsorption temperature rises, which is a consequence of the fact that the CO_2 physisorption is an exothermic process. The values of the heat of adsorption calculated by means of the Clausius-Clapeyron equation are ~ 24±2 $kJ \cdot mol^{-1}$, which is consistent with the data reported for CO_2 adsorption on porous carbons [33]. It is worth mentioning that the CO2 uptakes measured for the ATC samples presented here are substantially higher than those obtained for most of N-doped activated carbons designed for CO_2 capture [34, 35, 18]. However, it must also be indicated that the ATC carbons exhibit lower CO_2 capture capacities in relation to the chemically activated carbons prepared from pitch [19] and hydrothermally treated biomass [21].

3.3. Kinetics of adsorption, (CO₂/N₂) selectivity and sorbent regeneration

Efficient CO_2 capture from flue gases and other gas mixtures requires a sorbent that demonstrated not only a large CO_2 uptake but also fast adsorption kinetics, a good

selectivity towards CO_2 against other competing gases (i. e. N_2) and they must also be easy to regenerate. The performance of the activated templated carbons was assessed in the light of these pre-requisites. Fig. 6a shows the adsorption kinetics of CO_2 and N_2 in relation to the ATK-2-700 sample at 25 ºC. It can be seen that the capture of CO_2 takes place at high adsorption rates, more than 95% of the CO_2 being adsorbed in ~ 3 min. The N_2 adsorption occurs at a similar rate, but the amount of nitrogen adsorbed is considerably lower (~0.5 mmol N_2 g^{-1}). As a consequence, the $[CO^2/N^2]$ selectivity measured under equilibrium conditions shows a value of ~6.5, which clearly proves that

CO_2 and N_2 can be successfully separated by the activated templated carbons. This CO_2/N_2 selectivity is close to the selectivity values measured for other porous carbons used for CO_2 capture [19,21].

Easy regenerability is another requirement of CO_2 sorbents. The capacity of regeneration of activated templated carbons was tested by means of adsorption (CO_2 at 1 atm)–desorption (under helium) cycles carried out at room temperature (25 ºC). The results of these experiments for the ATK-2-700 sample are presented in Fig. 6b. It can be seen that the captured CO_2 is quickly desorbed after the gas carrier has been switched from CO_2 to He. In fact, >95% of the CO_2 is desorbed within 3 min under these conditions. This adsorption–desorption cycle was repeated six times and no noticeable changes were observed in the desorption kinetics or CO_2 uptake. Thus, the activated templated carbons reported here can be quickly, easily, and totally regenerated over multiple cycles without any loss of adsorption performance.

3. Conclusions

In summary, we have demonstrated that highly porous carbons obtained by chemical activation of templated carbons (i. e. CMK-3 and CMK-8) exhibit excellent properties as sorbents for CO_2 capture. The CO_2 adsorption properties, kinetics and regeneration of these materials were investigated. Regardless of the type of templated carbon used as precursor (CMK-3 or CMK-8), the activated samples exhibit similar CO_2 uptake capacities. The CO_2 capture capacities of the activated templated carbons are quite substantial (~ 3.2 mmol $CO_2 \cdot g^{-1}$ at 25 ºC) and hardly depend on the operation conditions used for the synthesis (i. e. reaction temperature or amount of activating agent). In other words, the CO_2 adsorption capacity of these activated carbons does not depend on their surface area but on the presence of narrow micropores (<1 nm). Furthermore, these porous carbons exhibit a high CO_2 adsorption rate, a good selectivity for CO_2–N_2 separation and they can easily be regenerated.

References

1. S. Rackley, *Carbon Capture and Storage*, Butterworth-Heinemann, Cambridge, **2009.**

2. Heinz-Wolfgang Häring, Christine Ahner, Industrial gases processing, p. 185, Wiley-VCH, Weinheim, 2008.

3. R. T. Yang, *Gas Separation by Adsorption Processes*, World Scientific Publishing Company, Boston, **1987**.

4. D. M. Ruthven, S. Farooq, K. S. Knaebel, *Pressure Swing Adsorption,* Wiley-VCH, New York, **1994**.

5. E. S. Kikkinides, R. T. Yang, S. H. Cho, *Ind. Eng. Chem. Res*. **1993**, *32*, 2714.

6. S. Sircar, T. C. Golden, M. B. Rao, *Carbon* **1996**, *34*, l.

7. R. V. Siriwardane, M.-S. Shen, E. P. Fisher, J. A. Poston, *Energy & Fuels* **2001**, *15*, 279.

8. B-K. Na, H. Lee, K-K. Koo, H. K. Song, *Ind. Eng. Chem. Res*. **2002**, *41*, 5498.

9. M. T. Ho, G. W. Allinson, D. E. Wiley, *Ind. Eng. Chem. Res*. **2008**, *47*, 4883.

10. R. E. Morris, P. S. Wheatley, *Angew. Chem. Int. Ed*., 2008, **47**, 4966.

11. S. Choi, J. H. Drese, C. W. Jones, *ChemSusChem,* 2009, **2**, 796.

12. N. Hedin, L. Chen, A. Laaksonen, *Nanoscale*, 2010, **2**, 1819.

13. S. Sircar, *Adsorption by Carbons*, Chapter 22 (Eds: E. Bottani, J. M. D. Tascón), Elsevier, New York, **2008**.

14. K. T. Chue, J. N. Kim, Y. J. Yoo, S. H. Cho, R. *T*. Yang, *Ind. Eng. Chem. Res.* **1995**, *34*, 591.

15. M. Radosz, X. Hu, K. Krutkramelis, Y. Shen, *Ind. Eng. Chem. Res.* **2008**, *47*, 3783.

16. M. M. Maroto-Valer, Z. Tang, Y. Zhang, *Fuel Process. Technol.* **2005**, *86*, 1487.

17. C. Pevida, M. G. Plaza, B. Arias, J. Fermoso, F. Rubiera, J. J. Pis, *Appl. Surf. Sci*. **2008**, *254*, 7165.

18. G-P. Hao, W-C. Li, D. Qian, A-H. Lu, *Adv. Mater.* **2010**, *22*, 853.

19. A. Wahby, J. M. Ramos-Fernandez, M. Martinez-Escandell, A. Sepulveda-Escribano, J. Silvestre-Albero, F. Rodriguez-Reinoso, *ChemSusChem* **2010**, *3*, 974.

20. M. Sevilla, P. Valle-Vigón, A. B. Fuertes, Adv Funct. Mater., DOI: 10.1002/adfm.201100291, 2011

21. M. Sevilla, A. B. Fuertes, Energy Environ. Sci. 2011, 4, 1765–1771.

22. Minkee Choi and Ryong Ryoo, J. Mater. Chem., 2007, 17, 4204–4209.

23. J. Górka, A. Zawislak, J. Choma, M. Jaroniec, Carbon 46 (2007) 1159

24. Kaisheng Xia, Qiuming Gao, Chundong Wu, Shuqing Song, Meiling Ruan, Carbon 45 (2007) 1989–1996.

25. W. Xing, C.C. Huang, S.P. Zhuo, X. Yuan, G.Q. Wang, D. Hulicova-Jurcakova, Z.F. Yan, G.Q. Lu, Carbon 47 (2009) 1715 –1722.

26. A.B. Fuertes, D.M. Nevskaia, Micropor. Mesopor. Mater. 62 (2003) 177.

27. Zhao D, Huo Q, Feng J, Chmelka BF, Stucky GD. J Am Chem Soc 1998;120:6024-36.

28. F. Kleitz, S. H. Choi, R. Ryoo, Chem. Commun. (2003) 2136.

29. Fuertes AB. Chem Mater 2004;16:449-55.

30. H. Marsh, F. Rodriguez-Reinoso, *Activated carbons*, Chp. 4, Elsevier, Amsterdam, 2006.

31. Shinae Jun, Sang Hoon Joo, Ryong Ryoo, Michal Kruk, Mietek Jaroniec, Zheng Liu, Tetsu Ohsuna, and Osamu Terasaki, *J. Am. Chem. Soc.* **2000,** *122,* 10712-10713.

32. Kamil P. Gierszal, Mietek Jaroniec, Tae-Wan Kim, Jeongnam Kim and Ryong Ryoo, New J. Chem., 2008, 32, 981–993.

33. S. Himeno, T. Komatsu, S. Fujita, *J. Chem. Eng. Data* 2005, **50***,* 369

34. J. Przepiorski, M. Skrodzewicz, A.W. Morawski, Appl. Surf. Sci. 225 (2004) 235.

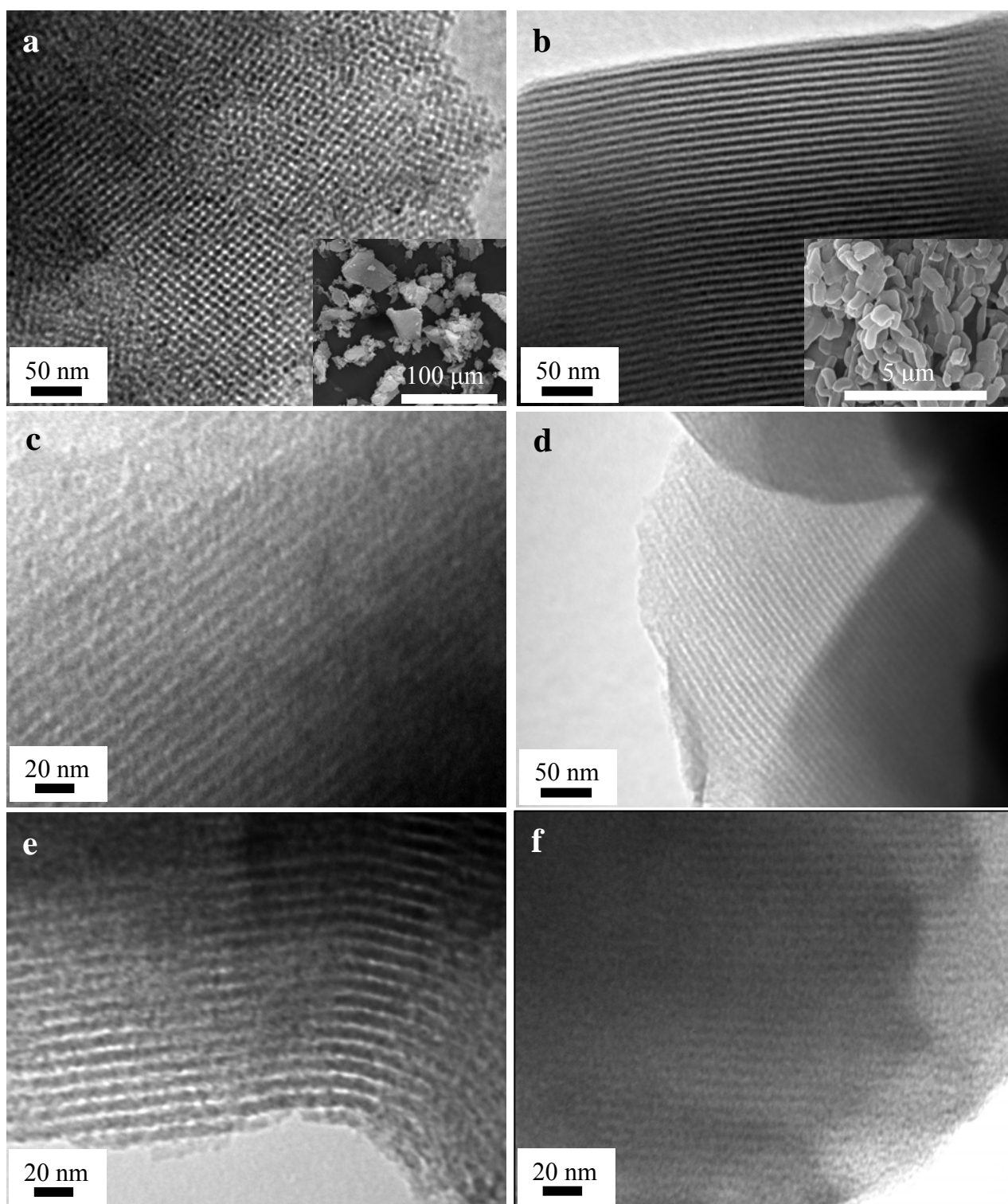35. C. Pevida, T.C. Drage, C.E. Snape, Carbon 46 (2008) 1464.

Figure 1. TEM images of: (a) CMK-8, (b) CMK-3, (c) ATK-2-600, (d) ATS-2-650, (e) ATS-2-700 and (f) ATS-2-800. Insets in (a) and (b) show the SEM images for the carbon samples CMK-8 and CMK-3 respectively.
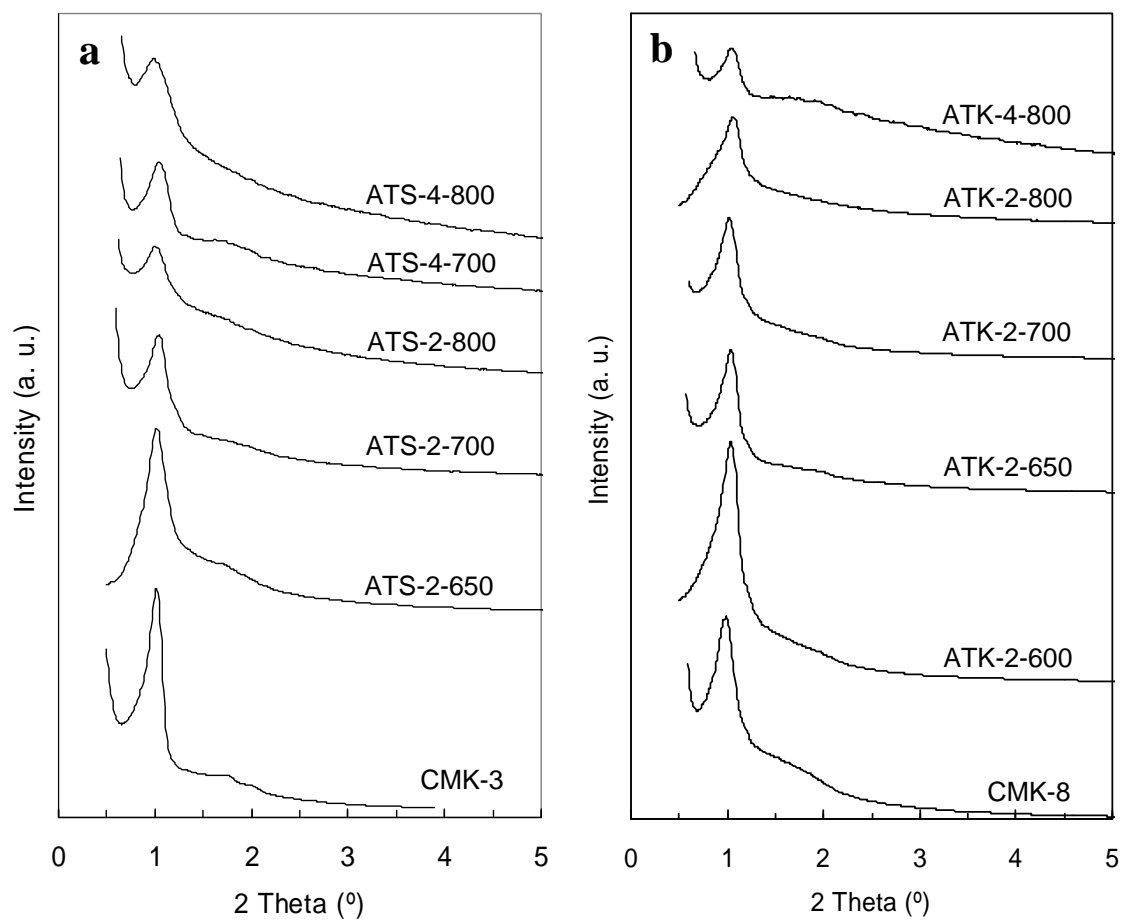
Figure 2. XRD patterns in the low-angle region for the activated templated carbons prepared from (a) CMK-3 and (b) CMK-8 mesoporous carbons.
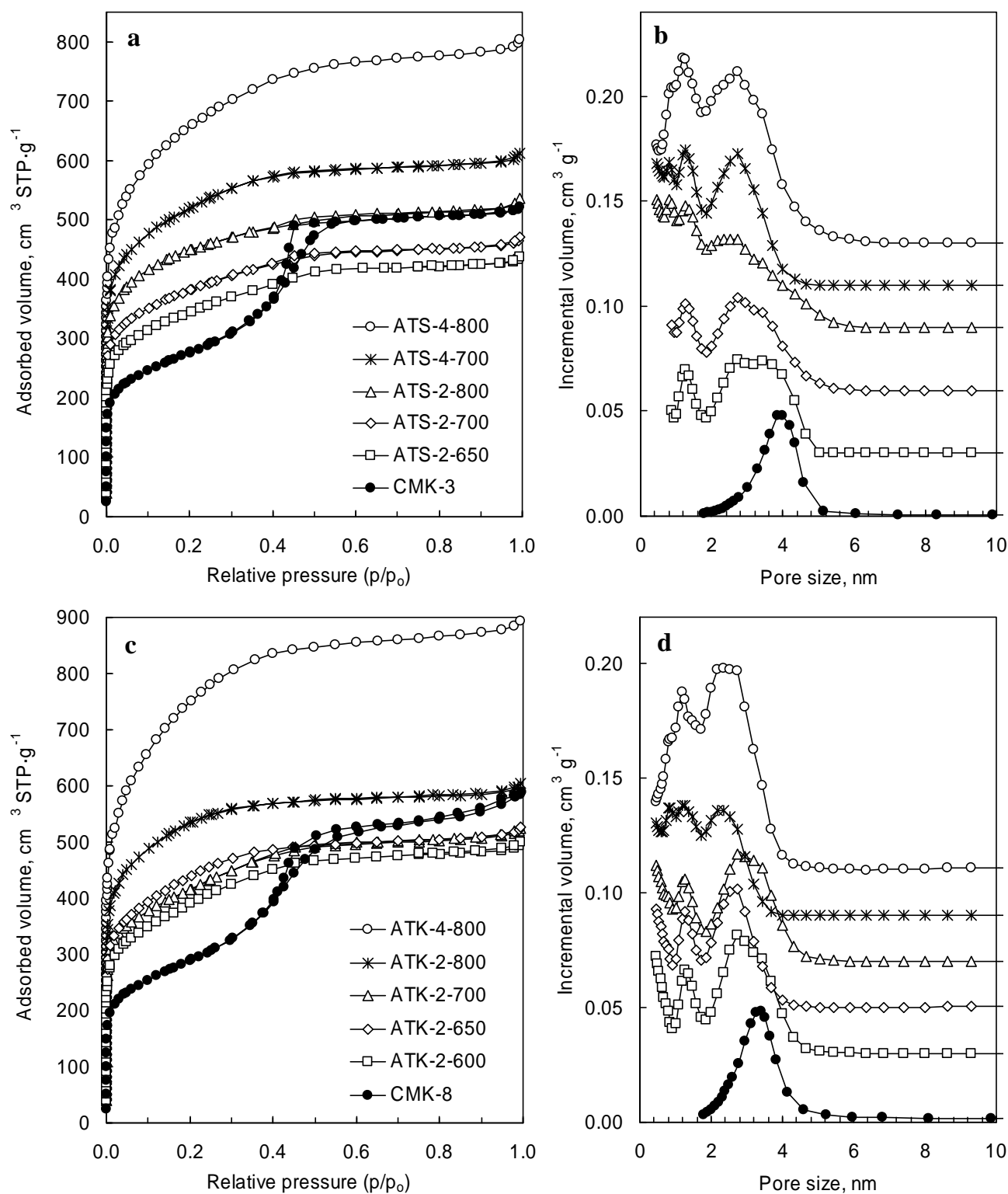
Figure 3. N$_2$ sorption isotherms (a, c) and pore size distributions (b, d) of activated templated carbons prepared from CMK-3 (a, b) and CMK-8 (c, d) samples.

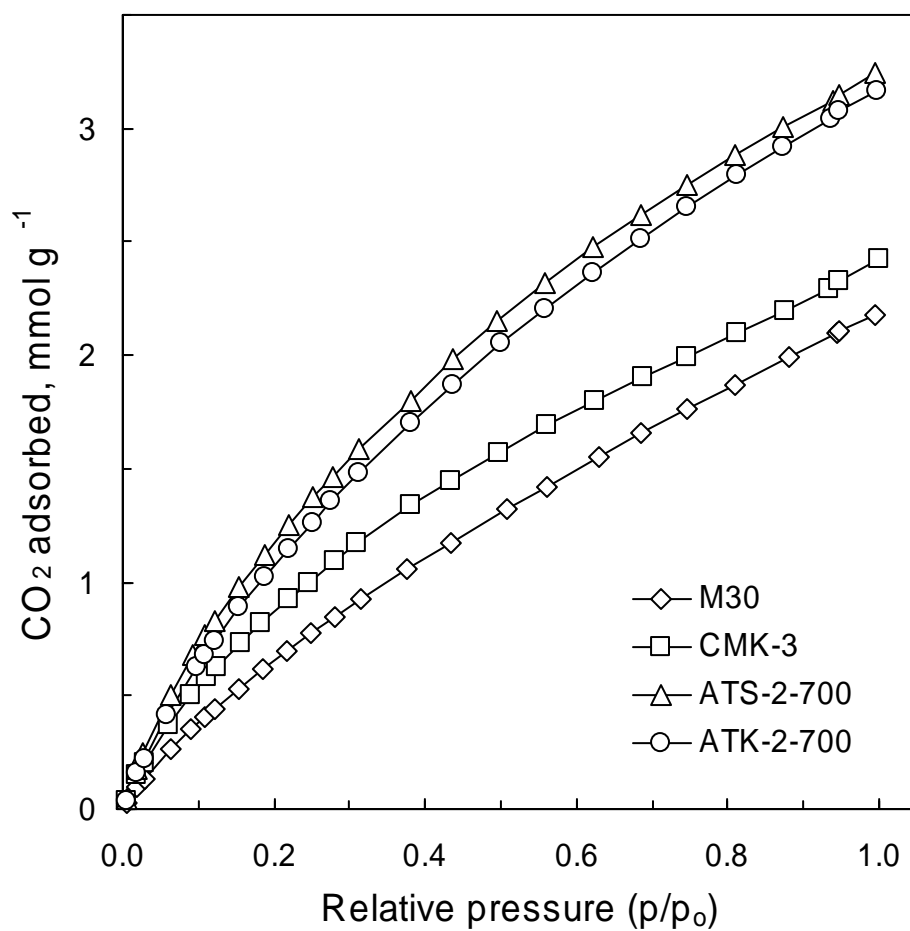**Figure 4.** CO_2 adsorption isotherms at 25 ºC for various porous carbon samples.
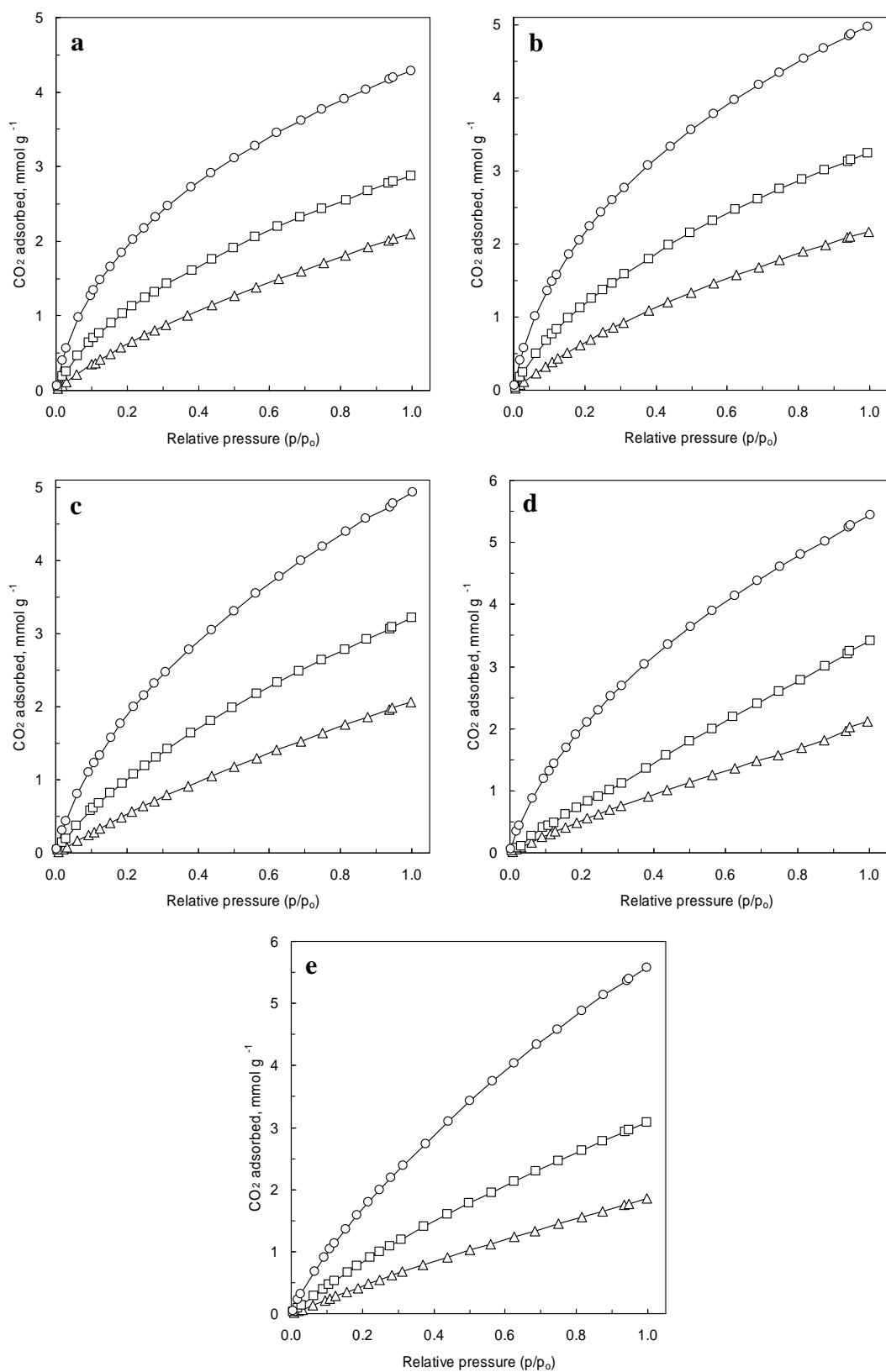
Figure 5. CO_2 adsorption isotherms at 0 ºC (Δ), 25 ºC (□) and 50 ºC (○) for the activated templated carbons obtained from CMK-3: (a) ATS-2-650, (b) ATS-2-700, (c) ATS-2-800, (d) ATS-4-700 and (e) ATS-4-800.
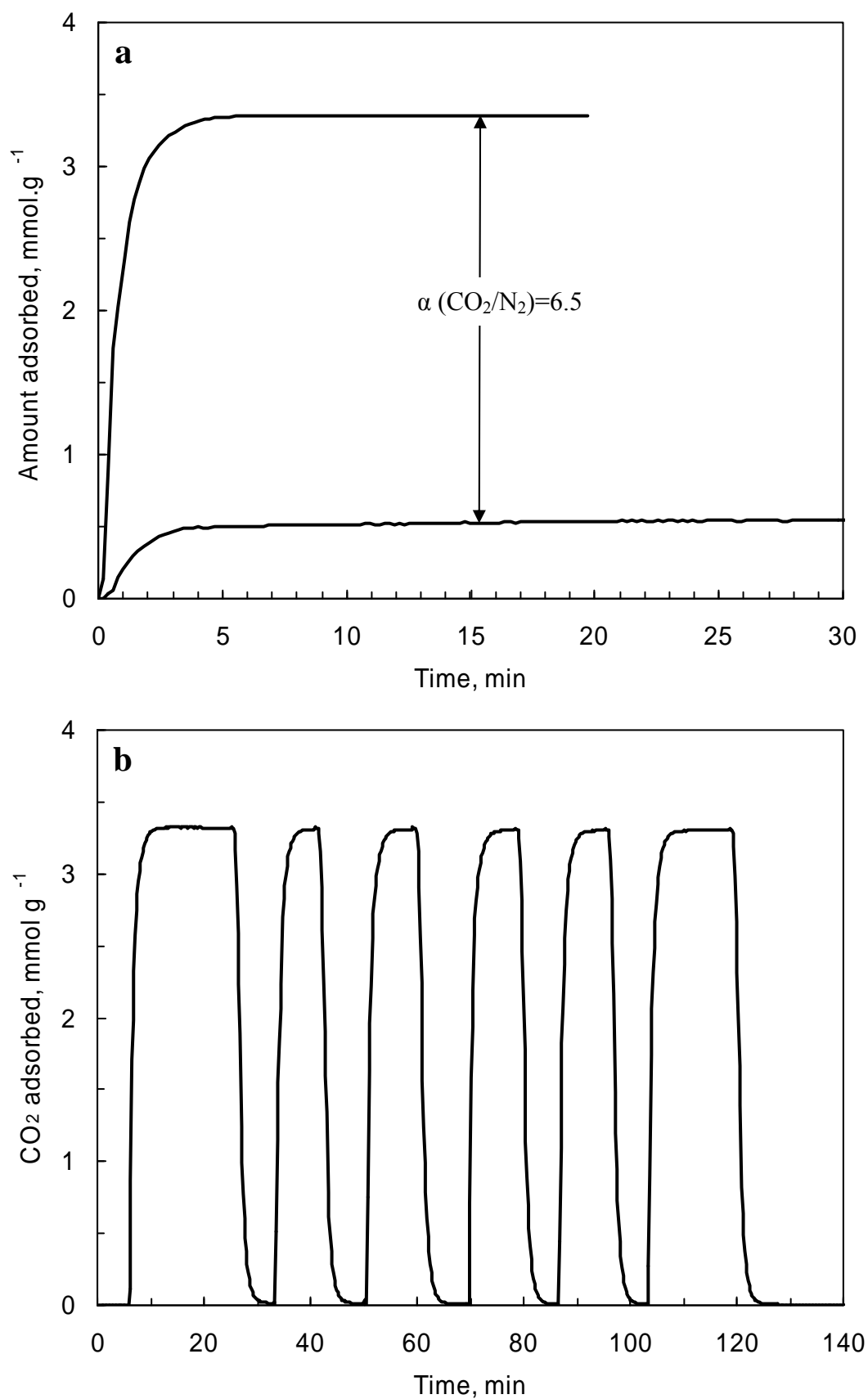
Figure 6. (a) Adsorption kinetics of CO_2 and N_2, and (b) CO_2 adsorption-desorption cycles obtained for the ATK-2-700 sample at 25 ºC (CO_2 concentration: 100 %).

21

Table 1. Textural properties of templated activated carbons.

Sample	S_{BET} [m^2 g^{-1}]	S_{micro} [m^2 g^{-1}] [a]	V_p [cm^3 g^{-1}] [b]	V_{micro} [cm^3 g^{-1}] [a]	Yield (%) [c]
M-30	2350	1510	1.51	0.79	-
CMK-3	970	260	0.81	0.12	-
ATS-2-650	1200	970	0.68	0.48	92
ATS-2-700	1330	1120	0.73	0.54	86
ATS-2-800	1570	1380	0.83	0.65	66
ATS-4-700	1820	1590	0.95	0.75	74
ATS-4-800	2310	1990	1.24	0.96	49
CMK-8	1020	-	0.91	-	-
ATK-2-600	1390	980	0.77	0.48	82
ATK-2-650	1545	1250	0.81	0.59	80
ATK-2-700	1450	1170	0.81	0.58	80
ATK-2-800	1870	1690	0.93	0.77	66
ATK-4-800	2660	2220	1.38	1.03	42

[a] Evaluated by the t-plot method. [b] Total pore volume at p/p$_o$ ~ 0.99. [c] Mass of activated carbon per 100 mass units of templated carbon.

Table 2. CO_2 capture capacities of the porous carbons at different adsorption temperatures and 1 atm.

Sample	CO_2 uptake, mmol·g^{-1} (mg·g^{-1})		
	0 ºC	25 ºC	50 ºC
M-30	3.8 (166)	2.2 (96)	1.6 (68)
CMK-3	3.2 (142)	2.4 (107)	-
ATS-2-650	4.3 (188)	2.9 (126)	2.1 (92)
ATS-2-700	5.8 (218)	3.3 (143)	2.2 (95)
ATS-2-800	4.9 (217)	3.2 (141)	2.1 (90)
ATS-4-700	5.4 (239)	3.4 (150)	2.1 (93)
ATS-4-800	5.6 (245)	3.1 (136)	1.9 (82)
CMK-8	-	2.1 (90)	-
ATK-2-600	4.9 (214)	3.0 (131)	2.6 (115)
ATK-2-650	5.0 (220)	3.0 (133)	2.0 (89)
ATK-2-700	5.2 (228)	3.2 (139)	2.0 (89)
ATK-2-800	5.3 (233)	3.2 (141)	2.0 (88)
ATK-4-800	5.4 (235)	3.1 (134)	2.0 (89)